17th Brazilian Congress of Thermal Sciences and Engineering
November 25th-28th, 2018, Águas de Lindóia, SP, Brazil

ENCIT-2018-0100
FAULT DETECTION AND DIAGNOSIS IN A REFRIGERATION SYSTEM USING THERMOECONOMIC METHODOLOGY AND ARTIFICIAL INTELLIGENCE

Tiago Mendes
Euler Guimarães Horta
Federal University of Jequitinhonha and Mucuri Valleys, Rodovia MGT 367 – Km 583, n° 5000, Alta da Jacuba, Diamantina-MG, 39100-000, Brazil
tiago.mendes@ict.ufvjm.edu.br
euler.horta@ict.ufvjm.edu.br

Osvaldo José Venturini
Marcelo José Pirani
Federal University of Itajubá, Av. BPS, n° 1303, 37500-093, Pinheirinho, Itajubá-MG, Brazil
osvaldo@unifei.edu.br
pirani@unifei.edu.br

Abstract. *The refrigeration systems are great consumers of electrical power in the commercial and industrial sector. Nowadays fault detection and diagnosis techniques, mathematical models and computer modelling have been used to improve the performance and predict behavior of refrigeration systems. Considering this scenario, the aim of this work is to apply a thermoeconomic methodology (the Fuel-Impact Formula, Malfunction and Dysfunction) for diagnosis. In addition, an artificial intelligence classifier was used to fault detection in the individual components based on measuring quantities of the system. It was analyzed the influence of each component malfunction in efficiency and power consumption of the system. Through this analysis, is possible to obtain a prognosis of the system behavior, as well as to perform a complete analysis of the whole refrigeration system and of each component.*

Keywords: *Thermoeconomic methodology, refrigeration system; computer modelling; artificial intelligence.*

1. INTRODUCTION

In the last years, the thermoeconomic methodology has been utilized to realize diagnosis in energy systems according to Piacentino and Catrini (2017). In the same way, the artificial intelligence has been utilized to realize fault detection and analyzes of operational behavior of the systems (Mulumba et al., 2015).

Through mathematical and computational modeling, several operating conditions of refrigeration systems can be simulated according to Mendes et al. (2017). Through these conditions can be calculated the thermoeconomic indices of the system and its components individually (Ommen et al., 2017). Properly structured artificial intelligence algorithm can be trained from previously known situations. With this algorithm can be realized predictions and generalizations with high reliability according to Kocyigit (2015).

2. METHODOLOGY

2.1 Cycle description and model

The operational behavior of a typical refrigeration system (Fig. 1) as a whole depends on its individual components (compressor, condenser, expansion device and evaporator) behavior. In this work, the simulation of the refrigeration system is conducted through the solution of a set of non-linear equations that governs the system operations, which were detailed in Mendes (2012). With the model development by Mendes (2012), one can obtain the refrigeration system behavior for various operational conditions, represented by different product storage conditions (T_{int}) and external ambient temperature (T_{ext}).

For the development of this model, it was necessary various information (design parameters) to represent each component of the system, and this information were obtained from their respective manufacturer catalogue data. The parameters obtained from the respective manufactures data are listed below:

- Volume displaced by the compressor ($\dot{V}_{desl}$);
- Isentropic (η_{isent}) and volumetric (η_{vol}) efficiencies of the compressor as a function of pressure ratio (RP);

- Capacity (heat transfer) per degree of temperature difference (C), for the condenser and evaporator, as a function of their respective air flows of fans;
- Maximum refrigerant mass flow rate ($\dot{m}_{fmax}$) provided by the expansion device (thermostatic valve);
- Coefficient characteristic (Ka) of the thermostatic valve.

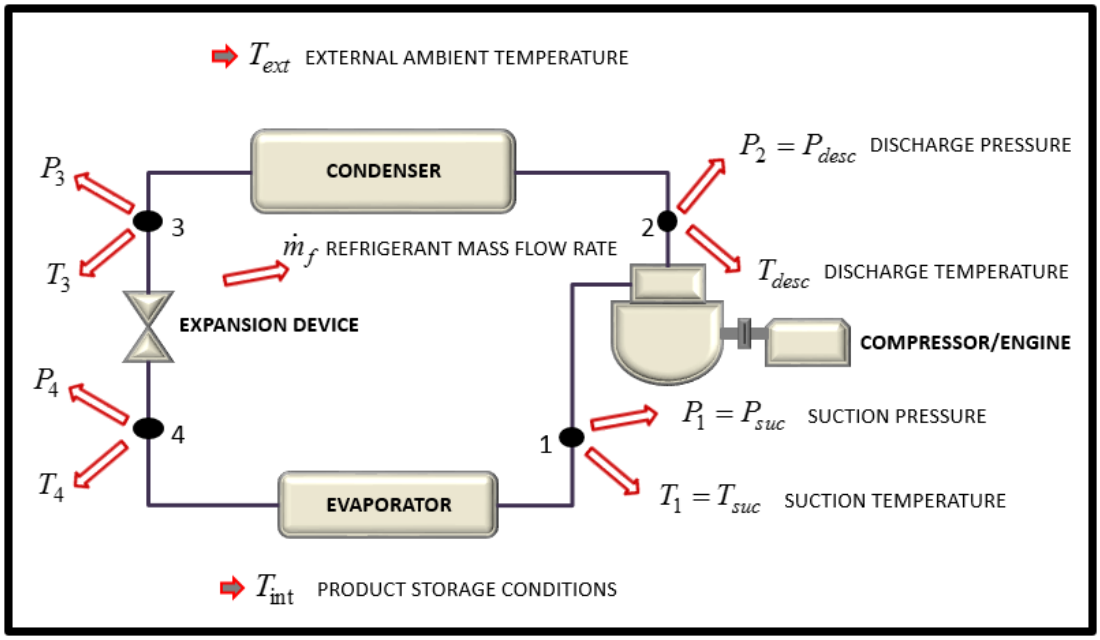

Figure 1. Simplified layout of a refrigeration system and representation of the measurements obtained in the same.

The presence of individual malfunctions in each component (compressor, condenser, expansion device and evaporator) will be represented in this work by:

- Reduction (-20%) of the isentropic efficiency of the compressor (η_{isent}). The inefficiency in compression simulates, for example, friction loss between the piston and the cylinder;
- Reduction (-25%) of the capacity (heat transfer) per degree of temperature difference (C) of the condenser. The objective is to simulate the presence of fouling (dust) on outer surface in the condenser, thereby reducing the coefficient of heat transfer;
- Reduction (-50%) in the coefficient characteristic (Ka) of the thermostatic valve used as expansion device. Inefficiency in the valve, for example, may be due to the obstruction in the flow of the refrigerant fluid there through, due to ice formation (presence of humidity in the refrigerant);
- Reduction (-25%) of the capacity (heat transfer) per degree of temperature difference (C), of the evaporator. The objective is to simulate the ice formation on the outer surface in the evaporator, thereby reducing the coefficient of heat transfer.

Using system operating data for various malfunctions and reference conditions (without malfunctions), it is possible to train a classifier to detect the presence of malfunction in the components of the refrigeration system. The behavior of these malfunctions, individually, will be assessed by measuring the following parameters of the refrigeration system, shown schematically in Fig. 1:

- External ambient temperature (T_{ext});
- Product storage temperature (T_{int});
- Suction pressure ($P_1 = P_{suc}$);
- Suction temperature ($T_1 = T_{suc}$);
- Discharge pressure ($P_2 = P_{desc}$);
- Discharge temperature ($T_2 = T_{desc}$);
- Pressure of point 3 (P_3);
- Temperature of point 3 (T_3);
- Pressure of point 4 (P_4);
- Temperature of point 4 (T_4);
- Refrigerant mass flow rate ($\dot{m}_f$).

These measurements are used in the artificial intelligence classifier for malfunctions detection and for thermoeconomic methodology for malfunctions diagnosis. The artificial intelligence classifier used will be detailed in the next section.

2.2 Fault detection using artificial intelligence classifier

The extreme learning machine (ELM) technique was developed for training the artificial neural networks. For networks such as ELM, the hidden layer parameters can be defined randomly, leaving only the weights of the output layer to be determined during training. These weights per time can be obtained numerically as a solution of a linear equations system. ELM is normally used in two layers, having the following characteristics (Horta, 2015):

- It have only one hidden layer with the number of neurons is large (Huang et al., 2006);
- Training the weights of the hidden layer and the output layer is done separately;
- The weights of the hidden layer are adjusted randomly;
- The weights of the output layer are not adjusted interactively, but are obtained directly using the pseudo-inverse method, without the need for interactions.

The measuring quantities of the system (pressures, temperatures and refrigerant mass flow rate) are used as input data for classifier in the Input Layer. These measuring quantities are in total 11 (eleven) and correspond to the dimensions of the classification problem The Output Layer is composed is of 5 (five) classes: reference conditions (without malfunctions); malfunction in compressor; malfunction in condenser; malfunction in expansion device and malfunction in evaporator. The topology for the problem of fault detection of the refrigeration system is shown in Fig. 2.

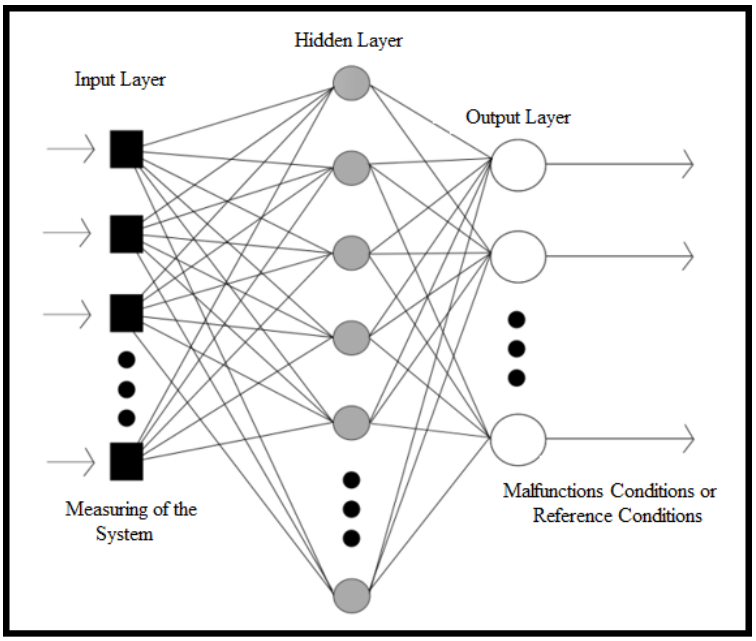

Figure 2. Topology of the ELMs for the fault detection.

The input matrix (X) for the ELM is presented in Eq. (1), which is composed of N patterns (lines) and n dimensions (columns).

$$X = \begin{bmatrix} X_1^T \\ \vdots \\ X_N^T \end{bmatrix} = \begin{bmatrix} x_{11} & \cdots & x_{1n} \\ \vdots & \ddots & \vdots \\ x_{N1} & \cdots & x_{Nn} \end{bmatrix} \tag{1}$$

The matrix H presented in Eq. (2) propagates the input matrix into a space larger than its dimension. H is formed by the activation function $g(x)$, where its weights (w) and bias (b) of the hidden layer are obtained randomly. In Eq. (3) the relation between the network output (T) and the matrix H is presented through a linear system. The matrix β corresponds to the solution for the linear system.

$$H = \begin{bmatrix} g \cdot (w_1 X_1 - b_1) & \cdots & g \cdot (w_p X_1 - b_p) \\ \vdots & \ddots & \vdots \\ g \cdot (w_1 X_N - b_1) & \cdots & g \cdot (w_p X_N - b_p) \end{bmatrix} \tag{2}$$

$$H\beta = T \tag{3}$$

The training process consists of propagating a training input matrix into the hidden layer of the ELM classifier. This results in the training matrix H and the linear system solution. The solution to the linear system is the matrix β that has the lowest norm and gives the least training error. After the training step the classification of a test input matrix can be performed. With known network parameters w, b and β, the classes of the test input matrix can be obtained. The class will correspond to the neuron index that has the highest activation value (Huang et al., 2006).

2.3 Exergy analysis to refrigeration system

In the application of thermoeconomics methodology, it is necessary the exergy analysis. For this analysis, the same measuring quantities in the refrigeration system shown in Fig. 1 are used. Additionally requires a mathematical formulation based on thermodynamics principles and mass conservation, and also the establishment of boundary conditions. The following considerations were taken into account in this work:

- For every condition, the system operates under quasistatic process each analyzed condition, and it may be considered to be on an equilibrium state (Bejan, 2006);
- "Heat losses" except in compressor (compression process is not isentropic) and expansion device are negligible;
- The kinetic and potential components of energy and exergy are also neglected.

The physical exergy of a mass flow (E_F) according to Bejan (2006), is given by Eq. (4), in which h_0 is specific enthalpy and s_0 is specific entropy, both at the dead state.

$$E_F = \dot{m}_f \cdot [(h - h_0) - T \cdot (s - s_0)] \tag{4}$$

where:
E_F: Physical exergy;
$\dot{m}_f$: Mass flow rate;
h: Specific enthalpy;
s: Specific entropy.

For some flows, the splitting of their physical exergy into its thermal (ET) and mechanical (EP) parts is necessary to better represent the flow into analysis (Morosuk and Tsatsaronis, 2008), as shown in Eq. (5) and Eq. (6), where specific enthalpy h_m and specific entropy s_m are calculated at pressure P (actual pressure point) and T_0 (temperature at the dead state).

$$ET = \dot{m}_f \cdot [(h - h_m) - T_0 \cdot (s - s_m)] \tag{5}$$

$$EP = \dot{m}_f \cdot [(h_m - h_0) - h_m \cdot (s_m - s_0)] \tag{6}$$

The exergy of heat flow ($B_{|Q}$) according to Bejan (2006) is given by Eq. (7).

$$B_{|Q} = \sum_j \left(1 - \frac{T_0}{T_j}\right) \cdot \dot{Q} \tag{7}$$

where:
$\dot{Q}$: Heat flow;
T_j: Temperature in the boundary (surface heat exchange).

The negentropy (S) according to Santos et al. (2009) is defined in the Eq. (8).

$$S = \dot{m}_f \cdot T_0 \cdot (s - s_0) \tag{8}$$

The temperature and pressure adopted for the dead state are, respectively, $T_0 = 20\,°C$ e $P_0 = 100\,kPa$. The determination of the properties h_0 and s_0 is based on these conditions.

2.4 Thermoeconomic analysis and diagnosis

The first step in the thermoeconomics analysis is the development of the productive structure of the plant being evaluated. The productive structure is constructed from the physical model and is made up of productive and dissipative

units (represented as squares), junction (rhombus) and bifurcation (circles). With regard to the condenser, in this work, the reduction of entropy of the refrigerant is considered as its product.

The splitting of physical exergy into its thermal and mechanical parts helps one to represent the product and input for component under analysis (Morosuk and Tsatsaronis 2008). These considerations lead to the productive structure shown in Fig. 3.

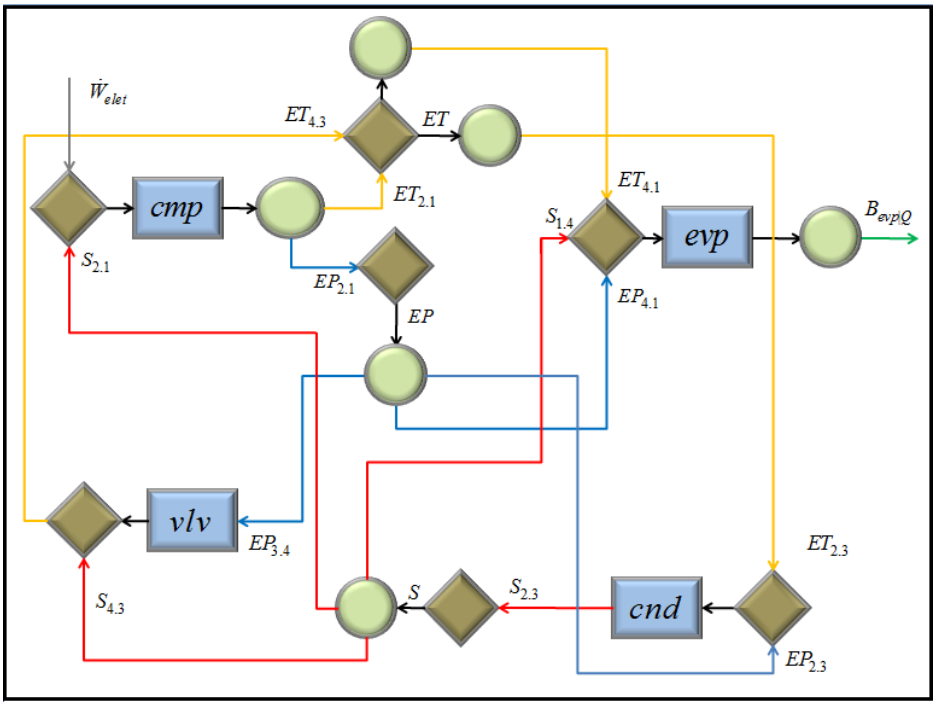

Figure 3. Productive structure of the refrigeration system of Fig. 1.

The productive structure is a graphical representation of the resources distribution over the whole thermal system. In this case, the system is considered to be composed of four productive units: compressor/engine (cmp), condenser (cnd), expansion device (vlv) and evaporator (evp), and three fictitious devices (bifurcation/junction): ET, EP and S.

The expansion device uses the flows $EP_{3.4}$ and $S_{4.3}$ as input, which are originated in the Bifurcation/Junction EP and S, respectively. The Bifurcation/Junction EP uses the $EP_{2.1}$ flow as input, which is originated in the compressor. The thermal component of the exergy flows $ET_{2.1}$ and $ET_{4.3}$ are considered as product of the compressor and expansion device, respectively. Both are the inputs for the Bifurcation/Junction ET, which provides the input flow $ET_{2.3}$ to the condenser and input flow $ET_{4.1}$ to the evaporator. Bifurcation/Junction S is responsible for allocating the product of the condenser (reduction of entropy). The condenser is responsible for the reduction of entropy generated by other components of the system. So, its product is allocated according to the entropy generated by each device.

The condenser heat flow $\dot{Q}_{cnd}$ does not have a useful destination for this system, thus it is not considered a product. The exergy flows $EP_{2.3}$ and $EP_{4.1}$, originated in the Bifurcation/Junction EP, are inputs to the condenser and evaporator, respectively. Finally, $B_{evp|Q}$ is the main product of the system, and $\dot{W}_{elet}$ is external input of the system. Once the state of the system has been determined, it is possible to obtain the Unitary Exergy Cost (k^*) for the all productive, dissipative and fictitious units that appear interrelated in productive structure shown in Fig. 4. The cost equations are arranged on a matrix form Fig. 4, and the resulting system of equation is solved to calculate Unitary Exergy Costs (k^*).

$$\begin{bmatrix} ET_{2.1}+EP_{2.1} & 0 & 0 & 0 & 0 & 0 & -S_{2.1} \\ 0 & S_{2.3} & 0 & 0 & ET_{2.3} & -EP_{2.3} & 0 \\ 0 & 0 & ET_{4.3} & 0 & 0 & -EP_{3.4} & -S_{4.3} \\ 0 & 0 & 0 & B_{evp|Q} & 0 & -EP_{4.1} & -S_{1.4} \\ ET_{2.1} & 0 & -ET_{4.3} & 0 & ET_{2.3}+ET_{4.1} & 0 & 0 \\ -EP_{2.1} & 0 & 0 & 0 & 0 & EP_{2.3}+EP_{3.4}+EP_{4.1} & 0 \\ 0 & -S_{2.3} & 0 & 0 & 0 & 0 & S_{2.1}+S_{1.4}+S_{4.3} \end{bmatrix} \times \begin{bmatrix} k_B^* \\ k_{cnd}^* \\ k_M^* \\ k_H^* \\ k_E^* \\ k_G^* \\ k_K^* \end{bmatrix} = \begin{bmatrix} \dot{W}_{elet} \\ 0 \\ 0 \\ 0 \\ 0 \\ 0 \\ 0 \end{bmatrix}$$

Figure 4: Equations system for calculating unit exergy costs.

The diagnosis method based on the Structural Theory of Thermoeconomics introduces the following parameters (Valero et al., 2006): Malfunction (MF) or the generation of the irreversibility increase, in Eq. (9); Dysfunction (DF) or the irreversibility of a component due to of alteration of its product, in Eq. (10); and the Fuel Impact or the Fuel-Impact Formula (ΔF_T), in Eq. (11). In order to bring together the problem of the impact of resources consumption with inefficiency diagnosis it is necessary to know the increase of the unitary exergy consumption. The Fuel Impact due to variation in the total product of the system ($\Delta F_{\Delta P}$) is defined by Eq. (12) (Valero et al., 2006).

$$MF = \sum(\Delta k) \cdot P^0 \tag{9}$$

$$DF = (k-1) \cdot \Delta P \tag{10}$$

$$\Delta F_T = MF + DF + \Delta F_{\Delta P} = \Delta\ {}^t k_e\ P^0 + \Delta\ {}^t k_p^* \Delta\langle KP\rangle P^0 +\ {}^t k_p^* \Delta P_S \tag{11}$$

$$\Delta F_{\Delta P} = k_p^* \cdot \Delta P \tag{12}$$

where:

Δk: Variation of unit exergy consumption;
P^0: Product vector in the reference state;
k: Unit exergy consumption;
ΔP: Variation of the product;
${}^t k_e$: Unit exergy consumption vector of the external input (transpose);
${}^t k_p^*$: Unit exergy cost vector of the product (transpose);
$\langle KP\rangle$: Matrix of unit exergy consumption;
ΔP_S: Variation in the total product of the system;
P_S: Final product vector;
k_p^*: Unit exergy cost of the product;
ΔP: Variation in the product;
P: Product.

3. RESULTS AND DISCUSSION

For the fault detection stage, the experiment was performed using the artificial intelligence classifier (ELM). The experiment consists in using the ELM to classify a certain operational condition represented for 11 (eleven) measuring quantities. These quantities are supposedly monitored in the refrigeration system and correspond to that dimensions of classification problem. In turn, each operational condition analyzed corresponds to a pattern of the classification problem. The proposed classification problem has 546 patterns and 11 dimensions. Of these 546 patterns, 42 correspond to reference conditions (without malfunctions) and the other 504 the conditions with individual malfunction in the components. For the network training, 1/3 of the total patterns were used, the remaining 2/3 were used for the test. This procedure was repeated 100 times, and the mean and standard deviation of the training and test accuracy were obtained. The training and test conditions were presented to ELM with 100 neurons in their hidden layer.

The Table 1 shows that the classifier correctly identified approximately 94% of the patterns presented in the test phase. In another words, the classifier was able to identify the class of the analyzed patterns in 94% of the cases. Once the problem classes are conditions without malfunction and with malfunction with distinction in that component. This result is considered satisfactory because the classifier was able the identification of the malfunction and the component where the malfunction of.

Table 1. Classifier accuracy for the first experiment.

Accuracy of the Training Set	0.945+/-0.005
Accuracy of the Test Set	0.937+/-0.013

After the fault detection stage in the available patterns, the fault diagnosis stage was performed in a pattern of each problem class. The fault diagnosis analysis was performed using the thermoeconomic methodology. This analysis using the same measuring used in the stage of fault detection by the ELM classifier.

The Input-Product (F-P) definition is represented for each component of the system, in Tab. 2, where F represents inputs (“fuel”) and P products. The components are evaluated by their Unit Exergy Consumption (k). The Table 3 shows the Unit Exergy Consumption of the components of the refrigeration system when operating at reference condition according to inputs and products defined in Tab. 2.

Table 2. Fuel-Product definition for productive structure.

N°.	Process Unit	Input (F)	Product (P)
1	Compressor/Engine	$\dot{W}_{elet} + S_{2.1}$	$ET_{2.1} + EP_{2.1}$
2	Condenser	$ET_{2.3} + EP_{2.3}$	$S_{2.3}$
3	Expansion Device	$EP_{3.4} + S_{4.3}$	$ET_{4.3}$
4	Evaporator	$ET_{4.1} + EP_{4.1} + S_{1.4}$	$B_{evp\|Q}$
5	Bifurcation/Junction ET	$ET_{2.1} + ET_{4.3}$	$ET_{2.3} + ET_{4.1}$
6	Bifurcation/Junction EP	$EP_{2.1}$	$EP_{2.3} + EP_{3.4} + EP_{4.1}$
7	Bifurcation/Junction S	$S_{2.3}$	$S_{2.1} + S_{1.4} + S_{4.3}$ [3]
-	Refrigeration System	$\dot{W}_{elet}$	$B_{evp\|Q}$

Table 3: Unit Exergy Consumption for the system components operating at reference condition.

Unit (Fig. 3a)	k [kW/kW]
Compressor/Engine (k_{cmp})	1.735
Condenser (k_{cnd})	0.085
Expansion Device (k_{vlv})	1.638
Evaporator (k_{evp})	15.037
Refrigeration System (k_{sist})	4.636

The exergy flow rates, the Exergy Costs and Unit Exergy Costs (k^*) at reference condition of the streams described in the productive structure of Fig. 3 are presented in Tab. 4.

Table 4: Thermoeconomic values for streams of Fig. 3.

Flow Exergy	Value [kW]	Exergy Cost	Value [kW]	Unit Exergy Cost	Value [kW/kW]	Description Flow
$ET_{2.1}$	9.110	$ET^*_{2.1}$	14.344	k^*_B	1.574	Thermal physical exergy
$EP_{2.1}$	13.330	$EP^*_{2.1}$	20.987	k^*_B	1.574	Physical exergy mechanical
$S_{2.1}$	4.265	$S^*_{2.1}$	0.670	k^*_K	0.157	Negentropy
$\dot{W}_{elet}$	34.662	$\dot{W}^*_{elet}$	34.662	k^*_{elet}	1.000	Exergy of power shaft
$ET_{2.3}$	9.236	$ET^*_{2.3}$	17.145	k^*_E	1.856	Thermal physical exergy
$EP_{2.3}$	0.038	$EP^*_{2.3}$	0.060	k^*_G	1.575	Physical exergy mechanical
$S_{2.3}$	109.572	$S^*_{2.3}$	17.205	k^*_{cnd}	0.157	Negentropy
$ET_{4.3}$	9.485	$ET^*_{4.3}$	20.174	k^*_M	2.127	Thermal physical exergy
$EP_{3.4}$	12.511	$EP^*_{3.4}$	19.700	k^*_G	1.575	Physical exergy mechanical
$S_{4.3}$	3.027	$S^*_{4.3}$	0.475	k^*_K	0.157	Negentropy
$ET_{4.1}$	9.359	$ET^*_{4.1}$	17.374	k^*_E	1.856	Thermal physical exergy
$EP_{4.1}$	0.780	$EP^*_{4.1}$	1.229	k^*_G	1.575	Physical exergy mechanical
$S_{1.4}$	102.280	$S^*_{1.4}$	16.060	k^*_K	0.157	Negentropy
$B_{evp\|Q}$	7.476	$B^*_{evp\|Q}$	34.662	k^*_H	4.636	Exergy of heat flow

The malfunctions in the compressor, condenser and evaporator leads to a reduction in the exergy flow $B_{evp|Q}$, which is related with the cooling capacity of the system (Tab. 5). The capacity reduction in the compressor and condenser increase the exergetic flow $\dot{W}_{elet}$, which is related with the energy consumption of the system (Tab. 5). The malfunction in the expansion device lead to a small variations in the exergy flow $B_{evp|Q}$ and $\dot{W}_{elet}$ (Tab. 5).

Table 5: Reference state and state with malfunctions in the compressor, condenser expansion device and evaporator.

Flow	$ET_{2.1}$	$EP_{2.1}$	$S_{2.1}$	$\dot{W}_{elet}$	$ET_{2.3}$	$EP_{2.3}$	$S_{2.3}$	$ET_{4.3}$	$EP_{3.4}$	$S_{4.3}$	$ET_{4.1}$	$EP_{4.1}$	$S_{1.4}$	$B_{evp\|Q}$
Reference State [kW]	9.110	13.330	4.265	34.662	9.236	0.038	109.572	9.485	12.511	3.027	9.359	0.780	102.280	7.476
Compr. (Insent.) [kW]	10.562	13.290	9.775	54.626	10.688	0.038	114.754	9.449	12.474	3.025	9.324	0.778	101.954	7.453
Condenser (dirt) [kW]	10.206	13.102	4.542	36.442	10.286	0.040	107.320	9.153	12.294	3.141	9.073	0.767	99.638	7.286
Ex. Device (K_a) [kW]	9.249	13.217	4.243	34.667	9.314	0.038	109.421	9.404	12.405	3.001	9.340	0.774	102.177	7.470
Evaporator (ice) [kW]	8.516	13.283	4.211	33.878	8.677	0.036	104.308	9.478	12.506	3.028	9.317	0.742	97.069	7.060

Table 6: Malfunction, Dysfunction, Fuel Impact, input and product of the system operating with the presence of malfunctions.

Malfunction	MF [kW]	DF [kW]	$\Delta F_{\Delta P}$[kW	ΔF_T [kW]	$\dot{W}_{elet}$ [kW]	$\dot{Q}_{evp}$ [kW]	$\Delta\dot{W}_{elet}$[kW]	$\Delta\dot{Q}_{evp}$[kW]	COP[kW]
Reference State	-	-	-	-	34.6	92.1	-	-	3.450
Compr. (Insent.)	22.635	-2.499	-0.172	19.964	54.6	91.8	19.964	-0.288	2.731
Condenser (dirt)	2.172	0.560	-0.951	1.780	36.4	89.8	1.780	-2.343	3.224
Ex. Device (K_a)	1.191	0.022	-1.997	-0.784	33.9	92.1	-0.784	-0.078	3.437
Evaporator (ice)	-0.006	0.040	-0.029	0.005	34.7	87.0	0.005	-5.130	3.345

The Tab. 6 shows the Malfunction, Dysfunction Fuel Impact obtained. For all the simulated malfunctions occurs changes in the thermoeconomic parameters presented, i.e., cause irreversibilities in the system. Finally, for each malfunction it was observed effects in the compression electrical power ($\dot{W}_{elet}$) and cooling capacity ($\dot{Q}_{evp}$), input and product of the refrigeration system, respectively. Therefore, there is a difference in the input ($\Delta\dot{W}_{elet}$) and in the product ($\Delta\dot{Q}_{evp}$) of the system due to the presence of malfunctions, Tab. 6. Also in the Tab. 6 it can be observed the reduction of the performance coefficient (COP) due to the tested malfunctions.

4. CONCLUSIONS

The fault detection and diagnosis of refrigeration system was conducted through artificial intelligence classifier and thermoeconomic methodology, respectively. In the fault detection stage, the classifier correctly identified the malfunction and the component where the malfunction is found, through measuring quantities of the system. This measuring quantities are the same used in themoeconomic diagnosis stage. In the diagnosis stage, occurs the concordance between the variation in the compression electrical power ($\dot{W}_{elet}$) and the Fuel Impact formula (ΔF_T). In a prognostic analysis, the effects on the coefficient of performance and cooling capacity are observed. Thus, to predicts the impact, for example, due to elimination of malfunctions.

5. ACKNOWLEDGEMENTS

The authors would like to express their gratitude to FAPEMIG, CAPES, CNPq, PRPPG/UNIFEI and PRPPG/UFVJM by the financial support that permitted the elaborations of this work, the ICT - Institute of Science and Technology/UFVJM and to NEST - Excellence Group in Thermal and Distributed Generation/UNIFEI by the physical and technical support.

6. REFERENCES

Bejan. (2006). Advanced Engineering Thermodynamics. New York: John Wiley & Sons, 3rd edition.

Horta. (2015). Aplicação De Máquinas De Aprendizado Extremo Ao Problema De Aprendizado Ativo. 87 f. Tese (Doutorado). Escola de Engenharia. Universidade Federal de Minas Gerais. Belo Horizonte.

Huang et al. (2006). Extreme Learning Machine: Theory And Applications. Neurocomputing, Vol 70, pp. 489–501.

Kocyigit. (2015). Fault and sensor error diagnostic strategies for a vapor compression refrigeration system by using fuzzy inference systems and artificial neural network. Intenational Journal of Refrigeration, Vol. 50, pp.69-79.

Mendes et al. (2017). Uso de um classificador para diagnóstico termodinâmico em um sistema de refrigeração. 13º Congresso Ibero-americano de Engenharia Mecânica, 13º Congreso Iberoamericano de Ingeniería Mecánica. Lisboa: CIBEM 2017 Lisboa, Portugal, 23-26 de Outubro de 2017.

Mendes, T. (2012). Diagnóstico Termodinâmico Aplicado a um Sistema de Refrigeração por Compressão de Vapor. Itajubá-MG: Dissertação Mestrado Unifei.

Morosuk and Tsatsaronis. (2008). A new approach to the exergy analysis of absorption refrigeration machines. Energy, Vol. 33, pp. 890–907.

Mulumba et al. (2015). Robust model-based fault diagnosis for air handling units. Energy and Buildings, Vol.86, pp. 698-707.

Ommen et al. (2017). Two Thermoeconomic Diagnosis Methods Applied to Representative Operating Data of a Commercial Transcritical Refrigeration Plant. Entropy, Vol. 19, 69-79.

Piacentino and Catrini. (2017). On Thermoeconomic Diagnosis of a Fouled Direct Expansion Coil: Effects of Induced Malfunctions on Quantitative Performance of the Diagnostic Technique. Journal of Sustainable Development of Energy, Water and Environment Systems, Vol. 05, Is. 2, pp. 177-190.

Santos et al. (2009). On the Negentropy Application in Thermoeconomics: A Fictitious or an Exergy Component Flow? International Journal of Thermodynamics, Vol. 12, N° 4, pp. 163-176.

Valero et al. (2006). Fundamentals of exergy cost. Accounting and thermoeconomics. Part I: Theory. Journal of Energy Resources Technology, Vol. 128, pp. 1-9.

7. RESPONSIBILITY NOTICE

The authors are the only responsible for the printed material included in this paper.